Dynamics of dense exciton gas in semiconductor nanocrystals

1997 J. Phys.: Condens. Matter 9 6771

(http://iopscience.iop.org/0953-8984/9/31/026)

J. Phys.: Condens. Matter **9** (1997) 6771–6780. Printed in the UK PII: S0953-8984(97)83521-7

Dynamics of dense exciton gas in semiconductor nanocrystals

G Tamulaitis†‡, S Pakalnis‡ and R Baltramiejūnas‡

† Institute of Materials Sciences and Applied Research, Vilnius University, Naugarduko 24, Vilnius 2006, Lithuania

‡ Institute of Physics, Goštauto 12, Vilnius 2600, Lithuania

Received 15 April 1997, in final form 27 May 1997

Abstract. The nonlinear absorption of CuBr nanocrystals embedded in a transparent glass matrix was investigated by using the excite-and-probe method. The luminescence properties of samples with different average nanocrystal radii were also studied. A fast-decaying damping of $Z_{1,2}$ exciton absorption band was observed, and interpreted as being mainly caused by elastic collisions between excitons. The relationship between the photoinduced changes of the absorption and the exciton density was established. Radiative exciton–exciton interaction and surface recombination were revealed as the main recombination processes governing the decay of excitons in CuBr nanocrystals, and the relevant rate constants were evaluated.

1. Introduction

Photogeneration of excitons in semiconductor materials causes large optical nonlinearities which can be utilized to investigate the dynamics of the exciton system, and exploited for processing the light beam in functional elements designed for various applications. In order to decrease the lifetime of the excitons, and, hence, to increase the operation rate of such nonlinear elements, it is beneficial to confine the excitons into small nanocrystals with large surface-to-volume ratios, causing intensive surface recombination. Furthermore, the materials consisting of semiconductor nanocrystals embedded in a transparent matrix are convenient for exciting a homogeneous exciton system in every nanocrystal with a weak decrease of exciton density through the thickness of the sample. When the nanocrystals are so small that their radii are comparable to the Bohr radius of the exciton in the semiconductor, new phenomena such as quantum confinement [1] and gigantic oscillator strength [2] occur, and these have been recently extensively investigated both theoretically and experimentally (see e.g. [3] for a review and further references). The modification of the absorption spectrum due to the excitation of a second electron–hole pair into such a small nanocrystal is thoroughly studied in [4], and further references are given therein.

The present paper presents results of a study of exciton systems in bulk-like nanocrystals, i.e. in nanocrystals where the influence of quantum confinement is not strong and a thermalized dense exciton gas can be photoexcited, provided that the critical density for the Mott transition to a plasma of free electron–hole pairs is not exceeded [5]. Such bulk-like nanocrystals provide an attractive opportunity to create a dense exciton system by using a level of excitation which is considerably lower than would be necessary for bulk crystal. The spatial diffusion of excitons that decreases the exciton density in bulk crystals and 2D structures is inhibited by the natural boundaries of nanocrystals.

0953-8984/97/316771+10$19.50

The nonlinear absorption caused by the exciton system has been investigated in CuCl [6–8] and CuBr [9] nanocrystals. Large optical nonlinearities due to biexciton formation were studied [6], and a bleaching of the excitonic absorption accompanied by a blue-shift of the lowest exciton absorption band was observed, and interpreted as being caused by the interaction of excitons, which cannot be treated as purely neutral bosonic quasiparticles when their density is strongly increased [7–9]. In spite of the extensive investigations of optical nonlinearities due to excitons in nanocrystals, the nanocrystal radius dependence of the nonlinear effects has scarcely been studied, especially towards the limit of bulk-like nanocrystals.

Extending our previous work [10], the present study is focused on exciton–exciton interaction in dense exciton gas, and surface recombination of excitons which was revealed by experiments on samples with nanocrystals of different radii. Copper bromide nanocrystals were chosen as the subject for investigation, since a comparatively large binding energy of excitons in CuBr ($E_B = 107$ meV) ensured the existence of excitons over a wide range of temperatures and exciton densities. In order to avoid the spectral hole-burning effect, we used a band-to-band excitation of the semiconductor. The excite-and-probe technique was utilized to investigate the time evolution of the nonlinear absorption, and the dynamics of the exciton system was also studied by measuring the luminescence spectra and their modification with increasing excitation intensity.

2. Experimental details

The CuBr nanocrystals were grown in a silicate glass matrix by using the diffusion-controlled process [1]. The average size of the nanocrystals was varied in a controlled manner by choosing appropriate heat treatment conditions, and checked by analysis of the low-temperature absorption spectra of the samples [1]. A set of six samples containing nanocrystals with different average radii ranging from 6 to 41.2 nm were fabricated under identical growth conditions, except that different annealing times were used.

Since the wavelength of the light used for the excitation and probing considerably exceeds the nanocrystal radii, the Maxwell Garnett theory can be applied in the description of the absorption of this composite material. The final result of the calculation of the dielectric function is that the absorption coefficient of the composite material is governed mainly by processes in semiconductor nanocrystals, while the influence of the matrix dielectric properties is greater on the reflection coefficient [11].

Furthermore, a laser excitation causes permanent changes in the absorption coefficient of the semiconductor-doped glasses [3]. It is plausible to assume that photomodification of the surface of the nanocrystals is the cause of the changes, but the detailed mechanism of the modification is still not understood. To avoid interference of the permanent changes in the absorption coefficient with the laser-induced transient absorption during our experiments, we initially exposed our samples to maximal excitation for a period sufficient for complete saturation of the absorption changes due to photomodification processes. For instance, for a sample containing nanocrystals of radius 14 nm, about 10 000 pulses of band-to-band excitation with a fluence of 10 mJ cm^{-2} were sufficient for completion of the permanent changes in the absorption. The further exposure to the excitation at the same or lower intensity changed neither the absorption nor the luminescence properties of the sample.

A passively mode-locked laser with $KGd(WO_4)_3$:Nd^{3+} crystal as an active medium, simultaneously generating 1.169 eV quanta and a Stokes component of stimulated Raman scattering at 1.050 eV, was utilized. The third harmonic of the Stokes component (quantum energy 3.15 eV, FWHM duration 5 ps) was used for excitation of the samples. In the

excite-and-probe experiments, the nonlinear absorption was probed by the radiation of a parametric generator pumped by the second harmonic of the original component of the $KGd(WO_4)_3$:Nd^{3+} laser radiation. The luminescence spectra were recorded in the time-integrated regime under the same excitation conditions and for the same configuration as in the excite-and-probe experiments.

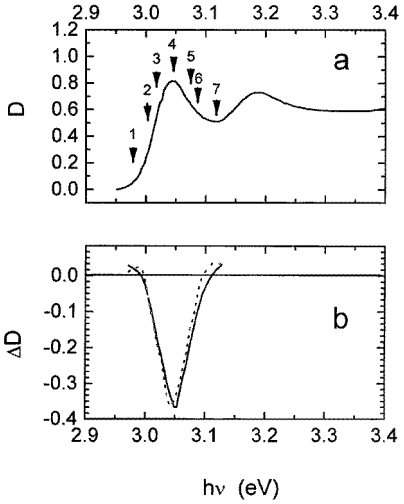

Figure 1. The optical density of a sample containing CuBr nanocrystals with average radius 6 nm (a), and the measured (full line) and calculated (dotted line) change of the optical density induced by photoexcitation (b). The energies of the probe quanta for the kinetics presented in figure 2 are indicated by arrows, and marked with corresponding numbers in (a).

3. Results

The spectrum of linear absorption of the sample with CuBr nanocrystals of 6 nm average radius is presented in figure 1(a). The two bands building the absorption edge of the sample can easily be identified by comparison with the absorption spectrum of bulk CuBr as caused by $Z_{1,2}$ (the low-energy band) and Z_3 excitons originating from the coupling of the lowest conduction band state Γ_6 to the both uppermost valence band holes Γ_8 ($Z_{1,2}$) and Γ_7 (Z_3) [12]. The bands are slightly blue-shifted due to the quantum confinement effect. The modification of the $Z_{1,2}$ exciton band due to photoexcited excitons is illustrated in figure 1(b). The kinetics of the transient absorption can be traced in figure 2 where the time evolution of the optical density is presented for several probe quantum energies indicated in figure 1(a). At zero delay between the exciting and probing beams, the optical density at the band peak drastically decreases, while induced absorption is observed in the wings of the band. So the behaviour of the band can be characterized as broadening without any shift of the band peak position. The nonlinear absorption completely relaxes within 50 ps after the excitation, without there being any traces of long-lasting decay components.

As has been discussed in [10], the observed damping of the band can be fairly well described by the broadening of a band with the Lorentzian shape. Then the relationship between the transient absorption coefficient $\Delta\alpha$ and the induced damping $\Delta\Gamma$ is simply

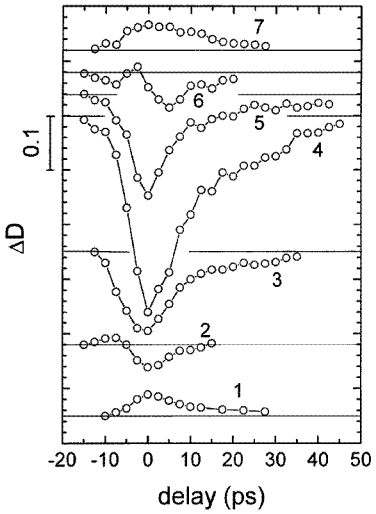

Figure 2. The time evolution of excitation-induced changes of optical density. The energies of the probe quanta for the kinetics presented are indicated, and marked with corresponding numbers in the spectrum of linear absorption in figure 1(a). Zero ΔD is indicated for each kinetics by a horizontal line, and a scale bar is provided to indicate the absolute value of ΔD.

expressed as

$$\Delta\alpha \propto \frac{[(\hbar\omega_0 - \hbar\omega)^2 - \Gamma^2 - \Gamma\,\Delta\Gamma]\Delta\Gamma}{[(\hbar\omega_0 - \hbar\omega)^2 + (\Gamma + \Delta\Gamma)^2][(\hbar\omega_0 - \hbar\omega)^2 + \Gamma^2]}. \tag{1}$$

The energy of the exciton resonance $\hbar\omega_0$ and the damping parameter Γ determined mainly by the inhomogeneous broadening due to the size distribution of the nanocrystals were obtained by fitting the Lorentzian shape to the $Z_{1,2}$ band in the spectrum of linear absorption.

Then the induced damping $\Delta\Gamma$ was estimated by fitting the expression (1) with the shape of the band of the excited sample. So the modification of the $Z_{1,2}$ band at the peak of the exciting pulse for the situation presented in figure 1(b) is best fitted by using $\Delta\Gamma = 20$ meV.

The damping of the band can be caused either by the heating of the lattice due to the absorbed laser energy or by the exciton–exciton interaction that intensifies with increasing exciton density. In order to distinguish between thermal and concentrational origins of the observed damping of the band, the dependence of the linear and nonlinear absorption on the lattice temperature was investigated. The modification of the edge of the linear absorption with increasing temperature is presented in figure 3. The blue-shift of the $Z_{1,2}$ exciton band with increasing temperature can be fairly well described by the Varshni formula [13]:

$$E(T) = E(0) - \gamma T^2/(T + \delta) \tag{2}$$

with empirical parameters $E(0) = 3.01$ eV, $\gamma = 1.80 \times 10^{-4}$ K^{-1}, and $\delta = 232$ K obtained by fitting the peak positions of the spectra presented in figure 3 with the expression (2).

The band also broadens with increasing temperature. We approximated the band-edge absorption with two Lorentzian-shaped bands corresponding to $Z_{1,2}$ and Z_3 excitons positioned in the Urbach tail of a band-to-band absorption. The dependence of the bandwidth Γ on the lattice temperature was approximated by

$$\Gamma(T) = \Gamma_0 + \beta_{ac}T + \beta_{LO}/(\exp(\hbar\omega_{LO}/k_BT) - 1). \tag{3}$$

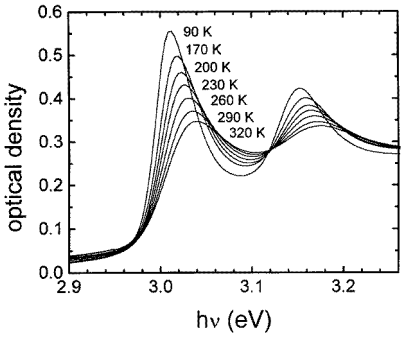

Figure 3. The optical density of CuBr-doped glass measured at the different temperatures indicated.

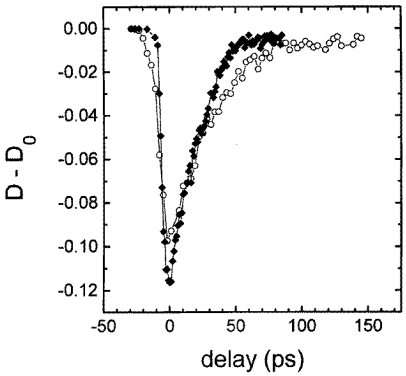

Figure 4. The time evolution of the transient optical density at room temperature (diamonds) and at 90 K (circles).

Here Γ_0 is the temperature-independent inhomogeneous broadening due to the size distribution of the nanocrystals, and the linear term reflects the influence of acoustic phonons, while the last term takes into account the scattering by longitudinal optical phonons with energy $\hbar\omega_{LO} = 21$ meV for CuBr. The experimentally obtained dependence is linear within the error of the Γ estimation which is complicated by slight asymmetry of the inhomogeneous broadening due to a Lifshitz–Slezov-type size distribution of the nanocrystals and the overlap of the $Z_{1,2}$ band with the Z_3 absorption band. Nevertheless we can conclude from the fitting that the influence of the third term in expression (3) is negligible up to the room temperature. The bandwidth is determined by the coefficients $\Gamma_0 = 25$ meV and $\beta_{ac} = 0.072$ K^{-1}.

The damping effect becomes slightly weaker and the recovery of the initial absorption lasts slightly longer when the temperature of the sample is decreased. The dynamics of the nonlinear absorption at 300 K and 90 K are compared in figure 4.

The kinetics of the transient absorption strongly depends on the average radius of the nanocrystals (see figure 5). The decay of the transient absorption is nonexponential in all of the samples under investigation. In the smallest nanocrystals, the time of complete recovery of the initial absorption is equal to $\approx$50 ps. When the average radius of the nanocrystals in the sample is in the range of tens of nanometres, the recovery occurs during the 200 to 300 ps after the excitation of the sample. It is worth noting that no slow decay components, however weak, were observed even by special investigation by using a set of pulses 5 ps long separated by 180 ps for excitation of the samples. The absence of the slow components is worth emphasizing as a distinctive peculiarity of CuBr nanocrystals. In nanocrystals of many other semiconductors, e.g. in CdS-doped semiconductor glasses, a component lasting for several nanoseconds was observed in the decay of the transient absorption [14]. So the optical nonlinearities in CuBr are appropriate for application in fast optical switches operating at a high repetition rate.

In order to complement the investigation of the nonlinear absorption, we also measured luminescence spectra under the same excitation conditions and for the same configuration as in the excite-and-probe experiments. The luminescence spectra at two excitation intensities are presented in figure 6, where the spectrum of linear absorption of the same sample with nanocrystals of radius 41.2 nm is also presented as a reference. The spectrum consists of a single band, which shifts with increasing excitation intensity to the low-energy side by up to

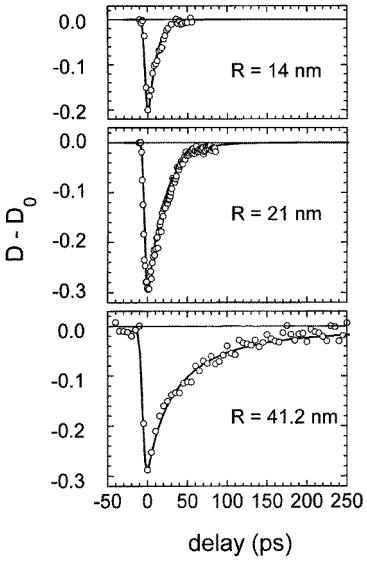

Figure 5. The time evolution of the transient optical density of samples containing nanocrystals with the different average radii indicated: experimental results (circles) and the best-fit calculated dependence (full line) discussed in the text.

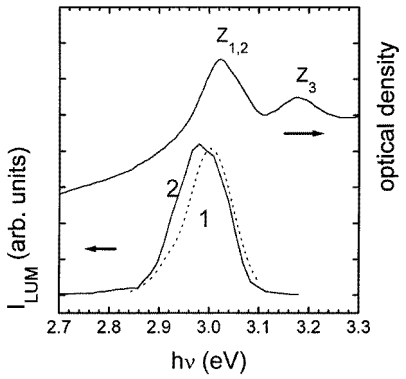

Figure 6. Luminescence spectra at excitation fluences of 0.06 mJ cm^{-2} (1) and 2 mJ cm^{-2} (2). The optical density of the sample is also presented for reference.

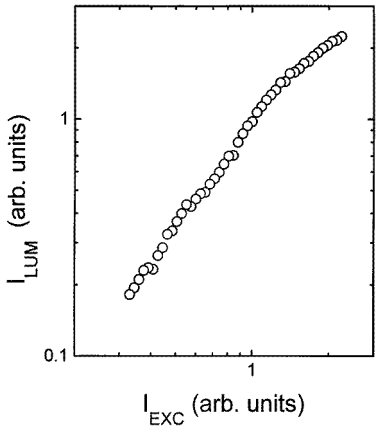

Figure 7. The excitation intensity dependence of the time-integrated intensity of the luminescence at the peak of its band.

40 meV from the position of the $Z_{1,2}$ exciton. The dependence of the luminescence intensity at the band peak on the excitation intensity is presented in figure 7. Two characteristic regions can be distinguished in this dependence. At the lowest excitation intensities, the dependence of the luminescence intensity on the excitation intensity is superlinear. The slope of the dependence decreases at a certain excitation intensity. The characteristics of the luminescence discussed are consistent with the increasing role of radiative exciton–exciton interaction, which prevails over the linear exciton recombination at the highest excitation intensities. The recombination occurs when a collision of two excitons results

in the recombination of one of the interacting excitons. The other interacting exciton remains in the excitonic state or dissociates to the excitonic continuum [15]. Because of the conservation of energy and quasi-momentum in the process, the corresponding luminescence band is peaked at the exciton energy or lower, depending on the final state of the interacting exciton which does not recombine. The lowest limit of the band peak position is at an exciton binding energy lower than the exciton energy [16]. As is usually observed for bulk semiconductors [17], the measured luminescence band is a superposition of the bands caused by radiative exciton–exciton interaction of different types. When the exciton density is increased, the contributions of the different processes to the total luminescence spectrum are rearranged, and this redistribution results in the shift of the band.

The excitation intensity dependence of the luminescence intensity is determined by the rate equation of the exciton density. In a quasi-steady state of the exciton system, the $I_L \propto I_{EXC}^2$ dependence corresponds to the situation when I_L reflects the luminescence due to radiative exciton–exciton interaction, while the recombination of excitons is dominated by a linear recombination (radiative and nonradiative). The dependence becomes linear when the radiative exciton–exciton recombination becomes dominant in both the luminescence and the exciton decay. The excitation pulse in our experiments was shorter than the instantaneous time constant of exciton decay, so the exciton system was not in a quasi-equilibrium state. However, the excitation intensity dependence of the time-integrated intensity of luminescence is close to that for quasi-steady conditions. So the observed dependence indicates the increasing role of the radiative exciton–exciton interaction when the exciton density is increased. This conclusion is also consistent with the transformation of the luminescence band with increasing excitation intensity discussed above.

4. Discussion

Summarizing the above-presented experimental results, we can conclude that the $Z_{1,2}$ exciton absorption band of CuBr nanocrystals is effectively damped by a band-to-band excitation. The relaxation of the transient absorption is faster than that in bulk CuBr, and strongly depends on the nanocrystal radius. Since the electron–hole pairs are generated in our experiments with a substantial excess energy with respect to the exciton state, the heating of the nanocrystal lattice has to be discussed as a possible cause of the damping. Furthermore, nonradiative recombination that is rather effective in semiconductor nanocrystals can be pointed out as another source of lattice heating. However, the experimental results indicate that the lattice is not heated during our experiment. According to equation (3) describing the temperature dependence of the damping constant of the band, an increase of temperature by 570 K is necessary to induce the change of damping constant $\Delta\Gamma = 20$ meV that was observed in the excite-and-probe experiment. Indeed, a contribution to $\Delta\Gamma$ from the third term in equation (3), which is negligible up to room temperature, can diminish the temperature necessary to cause the damping of 20 meV. Nevertheless, the temperature increase would be large enough to cause an observable shift of the band which, according to equation (2), would be 95 meV at $\Delta T = 570$ K. However, no shift of the band was observed in the experiment. Furthermore, it is hardly possible that such a substantial lattice heating decays within 100 ps after the excitation.

Consequently, the damping process is caused by collisions in the exciton system or by collisions of excitons with electrons. The latter possibility can easily be excluded by evaluating the ratio between densities of electrons (n_e) and excitons (n_{ex}) in our experiments. In the case of thermodynamic equilibrium between the exciton gas and free carriers, the

ratio of n_e to n_{ex} is described by the mass action law:

$$\frac{n_e^2}{n_{ex}} = \left[\frac{m_{de}m_{dh}k_BT}{2\pi\hbar^2 m_{dex}}\right]^{3/2} \exp\left[\frac{E_{ex}(n_e)}{k_BT}\right]. \tag{4}$$

Here T is the temperature, k_B is the Boltzmann constant, and m_{de}, m_{dh}, and m_{dex} are the effective masses of the density of states for electrons, holes, and excitons, respectively. The decrease of the exciton binding energy $E_{ex}(n_e)$ with increasing n_e can be evaluated from a corresponding expression for bulk crystals [18]:

$$E_{ex}(n_e) = E_R[1 - 1/g]\{\Phi(1-g) + [1-1/g]\Phi(g-1)\} \tag{5}$$

where E_R is the exciton rydberg, $\Phi(x)$ is the Heaviside function, and the parameter $g = 12/(\pi^2 a_B \kappa)$ is determined by the inverse screening length $\kappa^2 = e^2 n_e/(\varepsilon_0 \varepsilon k_B T)$, where ε_0 is the dielectric constant, and ε is the permittivity of the material.

At the maximum excitation level in our experiment ($\Delta t = 0$), when $n_{ex} + n_e$ equals $\sim 2\times 10^{18}$ cm^{-3}, the density of free electrons amounts to $0.1n_{ex}$ at the room temperature, and is negligible at the temperature of liquid nitrogen. However, the experiments on nonlinear absorption do not show any significant influence of temperature on the damping effect (see figure 4). So the densities of free electrons in CuBr under the conditions of our experiments are obviously too small to cause effective scattering of excitons. Consequently, the exciton–exciton collisions are the most plausible mechanism for the observed damping of the $Z_{1,2}$ exciton absorption band.

The elastic exciton–exciton collisions can be described by a classical model, if the condition

$$N\left[\frac{3}{2}\frac{M_{ex}}{\mu_{ex}}\frac{k_BT}{E_{ex}}\right]^{1/2} \gg 1 \tag{6}$$

is satisfied [19]. Here, M_{ex} and μ_{ex} are the translational and reduced masses of the exciton, and N a number indicating how much the typical impact radius exceeds the exciton Bohr radius. Since, for typical parameters of CuBr [20], the expression in brackets at room temperature equals 4, the above inequality may be assumed to be fulfilled. Then, according to the kinetic theory of gases, the change of the damping constant $\Delta\Gamma$ is in direct proportion to the exciton concentration:

$$\Delta\Gamma \approx 2ha_B^2(k_BT/M_{ex})^{1/2}n_{ex}. \tag{7}$$

The proportionality is convenient to utilize for evaluation of the dynamics of the exciton density, provided that $\Delta\Gamma$ has been measured. Since the energy of the exciton resonance $\hbar\omega_0$ and the damping parameter Γ contained in the expression (1) are easily obtained from the spectrum of linear absorption, then $\Delta\Gamma$, as the only dynamic parameter governing the excitation-induced changes of the absorption coefficient, can be calculated according to expression (1) by using the experimental data on $\Delta\alpha$. So the time-resolved measurement of $\Delta\alpha$ using the excite-and-probe method allowed us to follow the time evolution of the exciton density after the excitation.

The dynamics of the exciton density can be described by the rate equation

$$\frac{\mathrm{d}n_{ex}}{\mathrm{d}t} = G_0 \exp\left(-2.773\frac{t^2}{\theta^2}\right) - \left(\frac{1}{\tau} + \frac{3s}{R}\right)n_{ex} - Cn_{ex}^2. \tag{8}$$

The first term on the right-hand side of the equation expresses the rate of generation by a Gaussian-shaped laser pulse with full width at half-maximum (FWHM) θ (5 ps in our experiment). The second term describes the linear recombination. In addition to the lifetime τ reflecting the probability of linear recombination in bulk crystal, a term dependent

on the nanocrystal radius R is included. The term can be derived by treating the exciton motion in a nanocrystal in the same way as the free electron was treated in [21]. The rate of the exciton linear recombination at the nanocrystal surface is governed by the surface recombination velocity s. The third term on the right-hand side of equation (8) describes the rate of recombination due to radiative exciton–exciton interaction characterized by the constant C as a material parameter.

We fitted the time evolution of the transient absorption in seven samples containing CuBr nanocrystals with different average radii. The dynamics of the exciton density was calculated by solving equation (8). Then $\Delta\alpha$ at the band peak position was calculated by utilizing the direct proportionality of $\Delta\Gamma$ to n_{ex} described by expression (7). The fitting procedure fixed the surface recombination velocity s and the constant of radiative exciton–exciton interaction C for all seven samples. So the average nanocrystal radius obtained by independent characterization of the samples was the only specific parameter peculiar to different samples. Since the term characterized by the bulk lifetime τ turned out to be negligible in comparison with the R-dependent term of the linear recombination in the range of R of our samples, the recombination of excitons was governed mainly by the surface recombination at the lowest densities of excitons and the recombination due to exciton–exciton interaction prevailing in dense exciton gas. The calculated time evolution of $\Delta\alpha$ correctly describes the measured kinetics in all of the samples investigated, as is illustrated in figure 4, with $C = 2 \times 10^{-9}$ cm^{-3} s^{-1} and $s = 8 \times 10^4$ cm s^{-1} as the best-fit parameters. So the importance of radiative exciton–exciton interaction is demonstrated in correspondence with the interpretation of luminescence properties discussed above, and the constant of this interaction in CuBr is evaluated. The concurrence of this interaction with effective surface recombination in CuBr nanocrystals results in a rather fast decay of photoexcited excitons, and, consequently, a fast relaxation of the bleaching of the absorption band. Furthermore, the recombination rate can be intentionally designed by choosing the average radius of nanocrystals, though with some decrease in the absolute value of the nonlinear absorption in the smallest nanocrystals.

5. Conclusions

The damping of the absorption band of $Z_{1,2}$ excitons in CuBr nanocrystals is caused mainly by elastic collisions of excitons. The induced damping parameter is proportional to the density of excitons. So the exciton density can be estimated from the value of the transient absorption, and its time evolution can be revealed by time-resolved measurement of the nonlinear absorption. The dynamics of the exciton density was shown to be governed mainly by two recombination mechanisms: (i) by radiative exciton–exciton interaction resulting in recombination of one of the interacting excitons; and (ii) by surface recombination increasing with decreasing nanocrystal radius. The constant of radiative exciton–exciton interaction and the velocity of surface recombination in CuBr nanocrystals were evaluated by fitting the results of time-resolved measurements of transient absorption in samples containing nanocrystals with different average radii with the calculations based on the rate equation for the exciton density.

References

[1] Ekimov A I, Efros Al L and Onushchenko A A 1985 *Solid State Commun.* **56** 921
[2] Hanamura E 1988 *Phys. Rev.* B **37** 1273
[3] Yoffe A D 1993 *Adv. Phys.* **42** 173

[4] Park S H, Morgan R A, Hu Y Z, Lindberg M, Koch S W and Peyghambarian N 1990 *J. Opt. Soc. Am.* B **7** 2097
[5] Tamulaitis G, Juršėnas S, Kurilčik G and Žukauskas A 1997 *Superlatt. Microstruct.* at press
[6] Leonelli R, Manar A, Grun J B and Hönerlage B 1992 *Phys. Rev.* B **45** 4141
[7] Justus B L, Seaver M E, Ruller J A and Campillo A J 1990 *Appl. Phys. Lett.* **57** 1381
[8] Edamatsu K, Iwai S, Itoh T, Yano S and Goto T 1995 *Phys. Rev.* B **51** 11 205
[9] Henneberger F, Woggon U, Puls J and Spiegelberg C 1988 *Appl. Phys.* B **46** 19
[10] Tamulaitis G, Baltramiejūnas R, Pakalnis S and Ekimov A I 1993 *Superlatt. Microstruct.* **13** 199
[11] Rustagi K C and Flytzanis C 1984 *Opt. Lett.* **9** 344
[12] Goldmann A 1977 *Phys. Status Solidi* **81** 9
[13] Varshni Y P 1967 *Physica* **34** 149
[14] Baltramiejūnas R, Pakalnis S and Tamulaitis G 1992 *J. Cryst. Growth* **117** 622
[15] Benoît a la Guillaume C, Debever J-M and Salvan F 1967 *Phys. Rev.* **177** 567
[16] Moriya T and Kushida T 1976 *J. Phys. Soc. Japan* **40** 1668
[17] Baltramiejūnas R and Kuokštis E 1982 *Phys. Status Solidi* **111** 187
[18] Banyai L and Koch S W 1986 *Z. Phys.* B **63** 283
[19] Thomas G A, Frova A, Hensel J C, Miller R E and Lee P A 1976 *Phys. Rev.* B **13** 1692
[20] *Landolt–Börnstein New Series; Numerical Data and Functional Relationships in Science and Technology* 1982 Group III, vol 17, ed O Madelung (Berlin: Springer)
[21] Juršėnas S, Stepankevičius V, Strumskis M and Žukauskas A 1995 *Semicond. Sci. Technol.* **10** 302